Partial Contact Head-Disk Interface with Thermal Protrusion

Du Chen and David B. Bogy

Computer Mechanics Laboratory

Dept. of Mechanical Engineering

University of California

Berkeley, CA 94720

Abstract

A new partial contact head disk interface (HDI) with thermal protrusion is proposed for magnetic recording with densities of 1 Tbit/in^2 and above. This HDI has the advantage of maintaining light contact between the slider and the disk, so that both the bouncing vibration amplitude and the contact force are small compared with a traditional partial contact HDI. The slider's dynamic simulations are carried out to analyze the effect of various factors within the HDI, including the friction and adhesion between the slider and the disk, the track profile morphology on the disk and the air bearing design, on the slider's dynamic performance. It is found that the bouncing vibration amplitude can be reduced to as small as the flying height modulation (FHM) of a non-contact air bearing slider without thermal protrusion.

1. Introduction

Reducing the read/write transducer to disk spacing and hence the slider's flying height (FH) is required to achieve higher recording densities in hard disk drives. The Wallace spacing loss equation reveals that the magnetic signal decreases exponentially as the distance increases between the magnetic media and the read/write transducer. Reducing the flying height, or physical spacing, of the slider is necessary, since the protective layers- e.g. the slider and disk DLC and lubricant- must have certain minimum thicknesses for their performance. The maximum magnetic signal can be obtained at a spacing of zero, but this requires a contact recording interface.

Among those proposed interface designs such as wear-in and contact, a partial contact head disk interface (HDI), which relies on an air bearing film to support most of the suspension load, is a promising way to balance the requirements of low bouncing vibrations of the slider and low wear at the head. For full contact recording with a weak air bearing or without any air bearing [1], the vibration and wear of the slider are two obstacles for practical implementation. The wear-in HDI [2][3] may eliminate the mechanical-tolerance-related flying height modulation (FHM), however, damage to the read/write transducer in the wear-in process can not be eliminated and the transducer is also worn away. On the other hand, studies [4] [5] [6] on partial contact recording indicate that a small contact area is effective in reducing friction and slider bouncing.

This report presents a new partial contact HDI design to achieve a low transducer FH, low slider bouncing vibration, and a low contact force between the slider and disk.

This HDI makes use of the thermal protrusion feature of a thermal FH control (i.e. dynamic FH) slider, so that only the protrusion tip, close to the protruded transducer, contacts the disk surface. This report is focused on the study of the factors in the HDI affecting the slider's bouncing and slider-disk contact. An air bearing surface (ABS) design concept is proposed for the partial contact HDI with thermal protrusion.

2. Partial contact HDI with thermal protrusion

The thermal flying height control (TFC) or dynamic flying height (DFH) technique is widely used in current hard drives to lower the slider's FH, which is presented in the patent by Meyer et al [7]. This advantageous technique makes use of a resistance heating element near the read/write transducer. When a current is applied through the heating element, the Joule-heat-caused thermal expansion forms a local thermal protrusion close to the read/write transducer, which is near the trailing edge center. This local thermal protrusion reduces the flying height at the protruded transducer. In this way the transducer FH becomes adjustable. This technique not only provides control that can compensate for the static FH loss and reduce the likelihood of head-disk contacts for an air bearing slider, but also shows a potential of achieving a partial contact HDI.

With a heating power above a critical value in a properly designed slider, the thermal protrusion at the transducer comes into contact with the disk. The small contact area at the thermal protrusion tip, which has a radius of curvature around 20-30 mm and controlled by the input heating power, helps maintain light contact between the slider and the disk, while the rest of the ABS remains undeformed and

flies at a safe distance from the disk. Based on studies of the partial contact recording [5] [6], a small interference area between the slider and the disk results in small friction and contact force and small bouncing vibration. So it is expected that the performance of a partial contact slider with thermal protrusion is better than a partial contact slider with a micro trailing pad, such as that analyzed in [6].

3. Dynamic Simulation of a partial contact slider with thermal protrusion

The static simulation of an air bearing slider with thermal protrusion was first carried out by Juang, Chen and Bogy [8] with the consideration of the air bearing cooling effect. In the work of Chen and Bogy [9], HDI heat transfer models were implemented in the static simulation and the obtained static flying attitudes were compared. However, for the dynamic simulation of a partial contact slider with thermal protrusion on the disk surface, the thermal protrusion changes dynamically due to the dynamic air bearing cooling and the dynamic slider-disk interaction, which are associated with the slider's FHM or bouncing vibration. This dynamic thermal protrusion incurs difficulties in a full dynamic simulation of a partial contact slider with thermal protrusion.

In this report two approximations are adopted in the dynamic simulation. First, the thermal protrusion is taken as a constant geometry on the ABS, which only depends on the heating power for a given slider. This means that in the simulation the thermal protrusion does not change as the flying height modulates or the slider bounces on the disk surface. In fact, a transient thermal response study shows that the response of thermal protrusion has a bandwidth of about 1 kHz [8], which is much smaller than

the air bearing frequencies and bouncing frequencies. Hence, the first approximation is reasonable. Second, the friction heating and heat conduction caused by the slider-disk contact are negligible. In the slider-disk contact area, the friction heating counteracts the heat conduction from the slider to the disk. It is assumed in this report that the friction heating and contact-caused heat conduction cancel each other and the total effect is negligible, due to the small contact area at the tip of the thermal protrusion.

Based on these two approximations, two steps are taken for the dynamic simulation of a partial contact slider with thermal protrusion. First, the static flying attitude with thermal protrusion on a flat disk is calculated and the thermal protrusion profile is obtained for a given input heating power. The iteration approach in [8] with a static air bearing solver and a finite element analysis of thermal deformation is used. Second, the obtained thermal protrusion profile is added to the ABS profile and the dynamic simulation of the partial contact slider is carried out. A nonlinear dynamics model developed for a partial contact HDI in [6] is used here for the slider dynamics. The air bearing with contact and slider-disk adhesion, contact and friction are all considered in this model. As listed in [6], numerical methods are used to calculate the contact and adhesion force and solve the time-dependent air bearing equations and 3-degree-of-freedom slider dynamic equations.

In this report an INSIC pico slider with thermal protrusion, which was used in [8], is employed as Slider 1 in dynamic simulation. The slider's ABS is shown in Figure 1. We are interested here in studying the effects of various parameters on the

performance of partial contact sliders with thermal protrusion, and the pico form factor is suitable for that study, but we are not proposing a particular design for future use in HDDs, since the industry has already moved to the smaller femto form factor sliders. It has zero crown, camber and twist. The suspension preload is 1.5 gf and there is no load offset. The disk RPM is 7200. Another two sliders with the ABS's modified based on Slider 1 are used in the analysis of the effect of the ABS design on the slider's bouncing. A measured track profile, which is shown in Figure 2, is used in the dynamic simulation. Another rough disk track profile and burnished smooth track profiles are also used to analyze the effect of mico-waviness and roughness on the slider's bouncing. In the simulation the sliders are thermally actuated from 5 nm and a 1-ms dynamic simulation is carried out for the slider's response.

4. Simulation results and discussion of partial contact sliders with thermal protrusion

(1) FHM and bouncing vibration

The slider's transducer FH reduces as the heating power increases. Beyond a certain heating power, the slider may touch the disk surface. Figure 3 shows the time histories of the slider dynamics with heating powers from 0 mW, 15 mW, 20 mW to 25 mW. The slider flies above the disk surface when there is no heating. The 3-sigma of the variation of the transducer FH is 0.50 nm. When the heating power is increased to 15 mW, the slider touches the disk only at the beginning and the 3-sigma of the transducer FH is 0.57 nm. When the heating power is increased beyond 15 mW, the slider touches the disk surface and the minimum spacing becomes negative. The

3-sigma of the variation of the transducer FH increases to 1.06 nm at 20 mW and 1.04 nm at 25 mW. The bouncing vibration amplitude of the slider in partial contact is much larger than the FHM of the slider at flying. The mean pitch angle and roll angle decrease as the heating power increase, which agrees with the static simulation results in [9]. The variations of the pitch angle increase as the slider touches the disk. The contact force between the slider and the disk remains below 0.05 gf when the slider touches down, which is much smaller than the 1.5-gf preload of the suspension force acting on the slider.

Figure 3 also shows the corresponding power spectra of the FH with these values of heating powers. It is seen that the slider's peak frequencies increase as the slider flies lower with a heating power of 15 mW. This can be explained with the decreased FH and increased air bearing stiffness. When the slider touches the disk surfaces with heating powers above 20 mW, a high frequency peak around 700 kHz occurs. Similar to the high frequency peak of a partial contact micro-trailing pad slider, this high frequency peak is related to the slider-disk contact.

(2) A partial contact slider with thermal protrusion and a partial contact micro-trailing-pad slider

Figure 4 shows the time history of the dynamics of Slider 1 and the micro-trailing-pad slider in [6] on the smooth track in Figure 2. It is obvious that the vibration amplitudes of the transducer FH, pitch and roll of the micro-trailing-pad slider are much larger than those of Slider 1. The contact force of the micro-trailing-pad slider is also much larger than that of Slider 1. This indicates that

the contact between the disk and the protrusion tip, as opposed to that of the micro trailing pad, causes a smaller interaction between the slider and the disk. The slider's bouncing vibration and the contact force can be greatly reduced simultaneously through the partial contact with thermal protrusion.

(3) Friction between the slider and the disk

As discussed in [6], the friction force between a partial contact slider and a disk is not the direct cause of the slider's bouncing vibration, and it has only a slight effect on the bouncing amplitude. The reason is that the torque acting on the slider due to the friction force is much less than that from the contact and adhesion force, with respect to the slider's mass center. For the contact between the slider's thermal protrusion and the disk, it is expected that the effect of friction force is negligible, since the contact area and contact force is even smaller. This is verified by the dynamic simulation of Slider 1 with 25 mW heating power, as shown in Figure 5. Here the friction coefficient between the slider and the disk varies from 0.3, 1.0 to 2.0 and the disk track profile is that shown in Figure 2. The 3-sigma of transducer spacing remains approximately 1.0 nm. Also the vibrations of pitch and roll angles are almost the same as without friction considered. The contact force between the slider and the disk is also not affected by the friction coefficient. So the friction between the slider and the disk has almost no effect on the slider's bouncing vibration.

(4) Adhesion between the slider and the disk

The adhesion force between the slider and the disk is proportional to the change of surface energy before and after the slider-disk contact in the modified intermolecular

force model [10]. To study the effect of adhesion on the dynamics of Slider 1, the change of surface energy before and after contact is set to range from 0.08 J/m^2, 0.008 J/m^2 to 0.001 J/m^2. The disk track profile shown in Figure 2 is used and the heating power is 25 mW. The corresponding dynamic simulation results for Slider 1 are shown in Figure 6. As the change of surface energy varies, the vibration amplitudes of pitch and roll angles and the bouncing vibration amplitude do not change much. The 3-sigma of the transducer spacing ranges between 1.0-1.2 nm approximately. But the mean of transducer spacing increases from 1.66 nm, 1.98 nm to 2.01 nm, as the change of surface energy decreases. Correspondingly, the peak of the contact force decreases from 0.15 gf, 0.05 gf to 0.02 gf. This indicates that the slider-disk intermolecular adhesion has a smaller effect on the bouncing vibration of Slider 1 with thermal protrusion than of a partial contact slider with micro-trailing pad in [6]. The reason is related to the small contact area between the slider and the disk. As most parts of the ABS are farther away from the disk, the adhesion between them and the disk does not vary much. Reduced slider-disk adhesion only results in a higher transducer flying height and a smaller contact force, while the slider's bouncing vibration is almost unchanged.

(5) Disk surface

a. Rough disk surface and smooth disk surface

The smooth track profile shown in Figure 2 has a root mean square (RMS) value of 0.2 nm. A rough track profile with RMS 0.6 nm is shown in Figure 7. These two track profiles were obtained from the LDV-measured disk morphologies [14].

Frequency components below 10 kHz were filtered out and the profile features less than 5 μm could not be captured. These two tracks are incorporated into the dynamic simulation of Slider 1. To exclude the effect of slider-disk adhesion, the change of surface energy before and after contact is set as zero. The time histories of the slider dynamics are shown in Figure 8. The 3-sigma of the transducer spacing is around 3.5 nm on the rough track, while it is only around 1.0 nm on the smooth track. The peak of the contact force is 0.24 gf on the rough track, while it is only 0.02 gf on the smooth track. The vibration amplitudes of the pitch and roll angles are smaller on the smooth track than on the rough one. It is shown that a partial contact slider with thermal protrusion has a smaller contact force as well as bouncing vibration amplitude on a smoother disk surface. This agrees with the conclusion in [6] that the slider's bouncing is a forced vibration due to the micro-waviness and roughness moving through the HDI as the disk rotates. A smoother track has a smaller excitation and reduces the slider's bouncing vibration and contact force.

b. Burnished Disk Surfaces

As a further analysis of the effect of the track profile on the slider's bouncing, we numerically burnish the track profile shown in Figure 2. Here we employ two kinds of burnishing. One is a time-domain burnishing, which approximates the burnishing process of a glide-head slider on the track; the other is a frequency-domain burnishing, which is to show the effect of high frequency components of the track on the disk surface. For the time-domain burnishing, a smoothing method called running line smoothing [11] is used to burnish local peaks. This method carries out a linear fitting

between the measurement point position and the track profile height in the neighborhood of each measurement point. The linear fitting is taken as a base line at each point. The track is burnished where the track height is above the local base line. Here the neighborhood length is chosen to be 25 μm, which is approximately the length of the trailing pad of a glide-head slider. The remaining local peak height after burnishing is set as 0.1 nm, since local peaks may not be totally flattened after burnishing. The burnished track profile and power spectrum are shown in Figure 9(a). The frequency-domain burnishing is used to remove the components with frequencies higher than a given value from the track profile. Here that frequency is set to be 500 KHz. A low pass filter is used for this burnishing process. Figure 9(b) shows the burnished track profile and its power spectrum. In practice, the frequency-domain burnishing is hard to implement. The RMS values of the burnished tracks are still approximately 0.2 nm.

The time histories of Slider 1 with heating power 20 mW on the original track in Figure 2 and the burnished tracks in Figures 9(a) and (b) are plotted in Figure 10. The vibrations of the pitch and roll angles of Slider 1 on these three tracks are almost the same. However, the 3-sigma of the transducer FH is 1.1 nm on the original track, while it is 0.9 nm on the time-domain burnished track and 0.5 nm on the frequency-domain burnished track. However, the time history of the contact force remains almost unchanged. The removal of frequency components above 500 KHz reduces the bouncing vibration more than the removal of local peaks. As the external excitations above 500 KHz are removed, the bouncing vibration amplitude of Slider 1

can be lowered close to the FHM of Slider 1 without thermal protrusion. This is reasonable since the dominant frequencies of the slider's bouncing are around 700 kHz. This is also indicated by the power spectra of FH on these disk tracks. It is seen that the patterns of the power spectra are similar, however, the frequency peak around 700 kHz is much lower on the frequency-domain burnished track than on the unburnished or time-domain burnished track.

(6) ABS designs for a Partial Contact HDI with Thermal Protrusion

It has been shown by Thornton and Bogy [12] that the ABS design has an important effect on the slider's FHM. The ABS design with a high air pressure peak at the transducer helps reduce the slider's FHM [12]. Here we focus on the effect of the ABS design on the bouncing vibration of a partial contact slider, which has larger amplitude than the FHM of a flying slider. Two different ABS designs are obtained through modifying the ABS of Slider 1. The sliders with these two ABS's are denoted as Slider 2 and Slider 3, respectively, and they are shown in Figure 10. Slider 2 has no side trailing pads and Slider 3 has a small discrete trailing pad. With adjusted preload and load offset, the static flying attitudes of Slider 1, 2 and 3 can be very close. They are listed in Table 1.

The static simulations with and without heating power are carried out for these three sliders. The air bearing pressure profiles at the static state without heating power for Sliders 1, 2 and 3 are shown in Figure 11. It is seen from Figure 12 that Slider 2 has the highest air bearing peak pressure at the transducer and Slider 3 has the lowest peak pressure. The touch-down heating power is approximately 20 mW for Slider 1,

40 mW for Slider 2 and 10 mW for Slider 3. It is seen that Slider 3, which has the lowest peak air pressure at the transducer, has the smallest touch-down heating power, while Slider 2, which has the highest air bearing peak pressure at the transducer without side air bearing peaks, has the largest touch-down heating power. This agrees with the ABS design guideline for high actuation efficiency developed in [13]. The corresponding air bearing pressure profiles on touch-down are shown in Figure 13. Slider 2 still has the highest air bearing peak pressure. With the touch-down heating power, Slider 1 as well as Slider 2 has a dramatic increase in the air bearing peak at the transducer. However, the air bearing peak pressure at the discrete trailing pad of Slider 3 does not increase much after the heating power is on. This explains the small touch-down heating power of Slider 3.

With each touch-down heating power, the dynamic simulations of Slider 1, Slider 2 and Slider 3 are carried out, respectively. The time histories of the slider dynamics are shown in Figure 14. It is seen that the vibration amplitudes of the sliders are almost the same in the pitch and roll direction. However, the vertical vibration amplitudes of these sliders are different. The 3-sigma of the transducer FH is 1.0 nm for Slider 1, 0.7 nm for Slider 2 and 3.5 nm for Slider 3. The peak of the contact force is 0.5 gf for Slider 3, while it is less than 0.05 gf for Slider 1 and Slider 2. The plot of the minimum spacing shows that Slider 2 contacts the disk surface only from time to time. This indicates that the high air bearing pressure at the trailing edge center helps keep the slider in a light contact condition with the disk so that the contact force and bouncing amplitude also remain small.

5 Conclusions

A new partial contact head disk interface slider with thermal protrusion is analyzed to achieve a low transducer flying height for a high magnetic recording density. Light contact between the thermal protrusion tip, which is close to the protruded transducer, and the disk can be maintained with a certain heating power. A dynamic simulation scheme for such partial contact sliders with thermal protrusion is presented and discussed.

The results of the dynamic simulations show that the bouncing vibration amplitude and the contact force of a partial contact slider with thermal protrusion are much smaller than the partial contact mico-trailing pad slider on the same smooth disk track.

The dynamic simulation results also show the effect of various factors within the HDI, including the friction and adhesion between the slider and the disk, the track profile morphology on the disk and the air bearing design, on the slider's dynamic performance with thermal protrusion. It is found that the friction between the slider and the disk has almost no effect on the slider's vibration and mean flying attitude. The slider-disk adhesion changes the mean flying height, but has little effect on the slider's vibration. The slider's bouncing vibration amplitude can be reduced to a value similar to the FHM with no contact, when the disk track is burnished or the air bearing pressure peak is enforced at the trailing edge center. For the INSIC pico slider [8], the mean traducer flying height can be reduced below 3 nm with heating powers above 20 mW. The 3-sigma of the bouncing amplitude can be reduced from 1.1 nm to

0.5 nm, when the frequencies components above 500 Khz are removed from the track. A modified air bearing surface with a higher air bearing pressure at the transducer weakens the contact force between the protrusion tip and the disk, while the bouncing vibration amplitude is only 0.5 nm, which is comparable to the flying height modulation of the INSIC slider without thermal protrusion, and the peak of the contact force is less than 0.05 gf, which is much smaller than the suspension preload.

Acknowledgement

This research was supported by the Information Storage Industry Consortium (INSIC) and the Computer Mechanics Laboratory (CML) at the University of California at Berkeley.

References

[1] J. Itoh, Y. Sasaki, K. Higashi, H. Takami and T. Shikanai, "An experimental investigation for continuous contact recording technology," *IEEE Trans. Magn.*, vol. 37, no. 4, pp. 1806–1808, Jul. 2001.

[2] B. Strom, S. Deits, C. Gerber, D. Krajnovich, D. Ohlsen and R. Turner, "Burnishing heads in-drive for higher density recording," *IEEE Trans. Magn.*, vol. 40, no. 1, pp. 345–347, Jan. 2004.

[3] G. P. Singh, B. E. Knigge, R. Payne, R. H. Wang, C. M. Mate, P. C. Arnett, C. Davis, V. Nayak, X. Wu, K. Schouterden and P. Baumgart, "A novel wear-in-pad approach to minimizing spacing at the head/disk interface," *IEEE Trans. Magn.*, vol. 40, no. 4, pp. 3148–3153, Jul. 2004.

[4] C. M. Mate, P. C. Arnett, P. Baumgart, Q. Dai, U. M. Guruz, B. E. Knigge, R. N.

Payne, O. J. Ruiz, G. J.Wang and B. K. Yen, “Dynamics of contacting head-disk interfaces,” *IEEE Trans. Magn.*, vol. 40, no. 4, pp. 3156–3158, Jul. 2004.

[5] J. Xu, H. Kohira, H. Tanaka and S. Saegusa, “Partial-Contact Head-Disk Interface Approach for High-Density Recording,” *IEEE Trans. Magn.*, vol. 41, no. 10, pp. 3031–3033, Oct. 2005.

[6] D. Chen and D. B. Bogy, “Dynamics of Partial Contact Head Disk Interface,” *IEEE Trans. Magn.*, vol. 43, no. 6, pp. 2220-2222, Jun. 2007

[7] D. W. Meyer, P. E. Kupinski and J. C. Liu, “Slider with temperature responsive transducer positioning,” U. S. Patent 5991113, Nov., 1999.

[8] J. Y. Juang, D. Chen and D. B. Bogy, “Alternate air bearing slider designs for areal density of 1 Tbit/in^2”, *IEEE Trans. Magn.*,vol. 42, No. 2, pp. 241-247, 2006.

[9] D. Chen and D. B. Bogy, “Simulation of static flying attitude with different heat transfer models for a flying height control slider with thermal protrusion,” Technical Report No. 2008-03, Computer Mechanics Laboratory, Department of Mechanical Engineering, University of California, Berkeley, 2008.

[10] D. Chen and D. B. Bogy, “Intermolecular force and surface roughness models for air bearing simulations for sub-5nm flying height sliders,” Technical Report No. 2006-016, Computer Mechanics Laboratory, Department of Mechanical Engineering, University of California, Berkeley, 2006.

[11] L. Fahrmeir and G. Tutz, *Multivariate Statistical Modelling Based on General Linear Models*, second edition, Springer, 2001.

[12] B. H. Thornton, A. Nayak and D. B. Bogy, “Flying height modulation due to

disk waviness of sub-5 nm flying height air bearing sliders," *ASME Jour. of Tribol.*, vol. 124, No. 4, pp. 762-770, 2002.

[13] J. Y. Juang and D. B. Bogy, "Air-bearing effects on actuated thermal pole-tip protrusion for hard disk drives," *ASME Jour. of Tribol.*, vol. 129, No. 3, pp. 570-578, 2007.

[14] B. H. Thornton, D. B. Bogy and C. S. Bhatia, "The effects of disk morphology on flying-height modulation: experiment and simulation," *IEEE Trans. Magn.*, vol. 38, No.1, pp. 107–111, Jan., 2002.

Table 1 Suspension load and flying attitudes of Slider 1, 2 and 3 with heating power off

	Suspension load	Flying attitude
Slider 1	Preload: 1.5 gf X-offset: 0 nm Y-offset: 0 nm	Transducer FH: 4.60 nm Pitch: 187.31μrad Roll: -0.57μrad
Slider 2	Preload: 1.8 gf X-offset: 200 nm Y-offset: 0 nm	Transducer FH: 4.46 nm Pitch: 169.40μrad Roll: 1.59μrad
Slider 3	Preload: 1.1 gf X-offset: 50 nm Y-offset: 0 nm	Transducer FH:4.87 nm Pitch: 179.60 μrad Roll: -1.70μrad

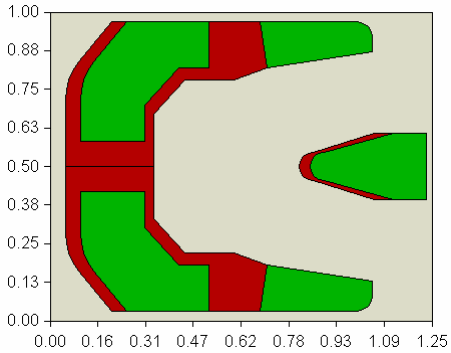

Fig.1. Air bearing surface of Slider 1 (unit: mm).

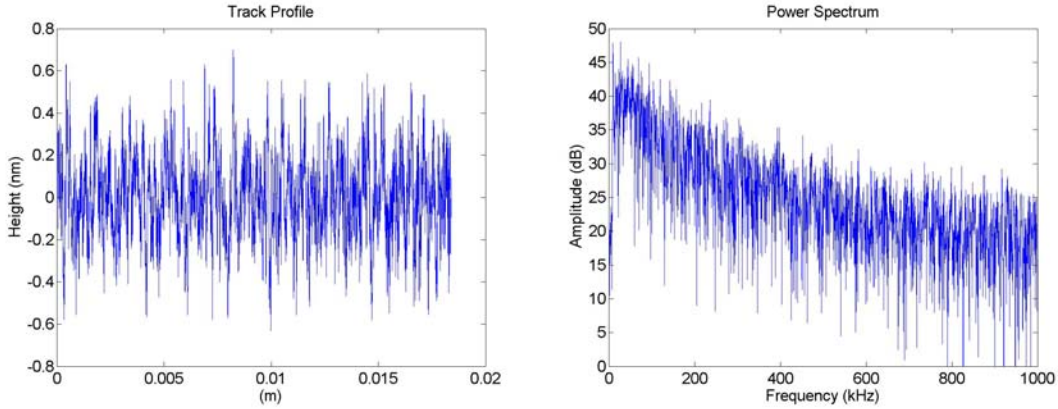

Fig.2. A smooth track profile and its power spectrum corresponding to a disk linear velocity of 17.34 m/s.

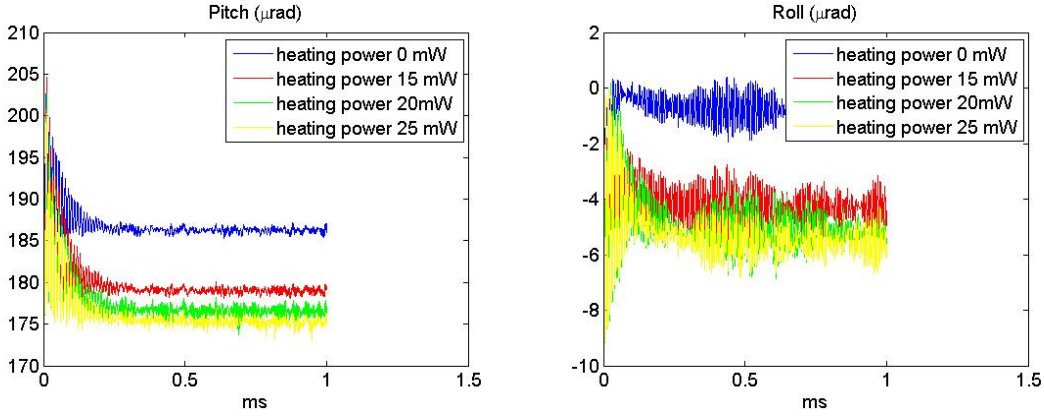

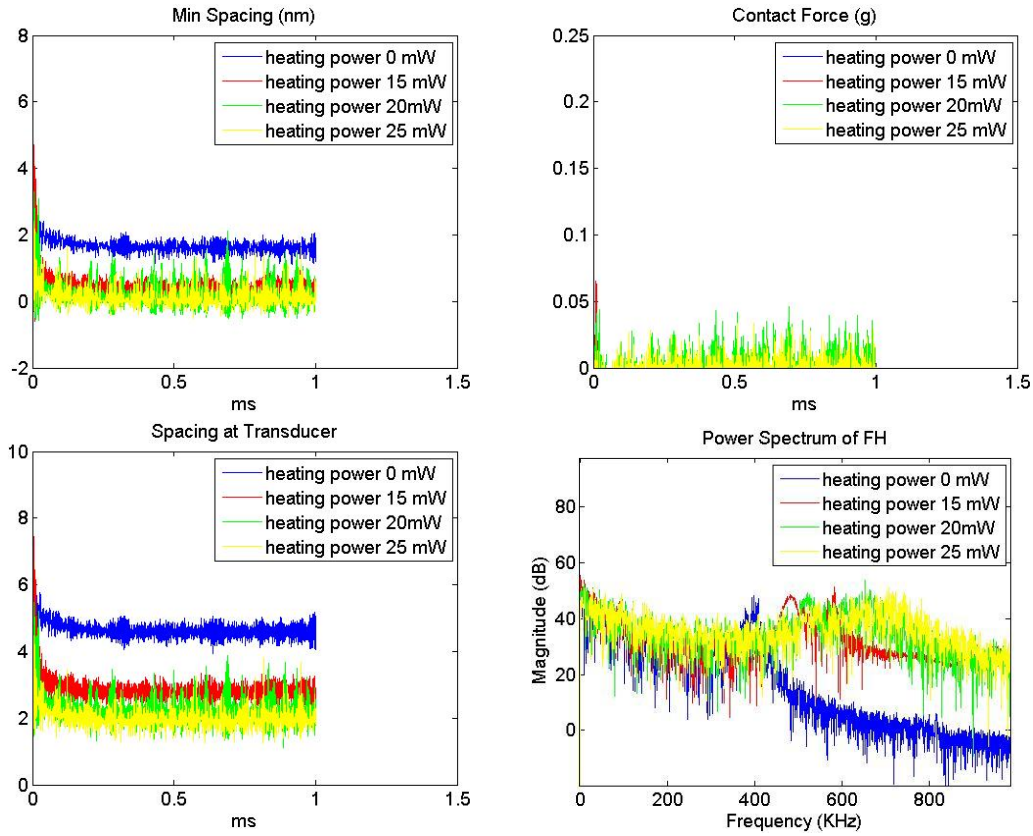

Fig.3. Time history of Slider 1 with heating powers of 0 mW, 15 mW, 20 mW to 25mW and the corresponding FH power spectrum.

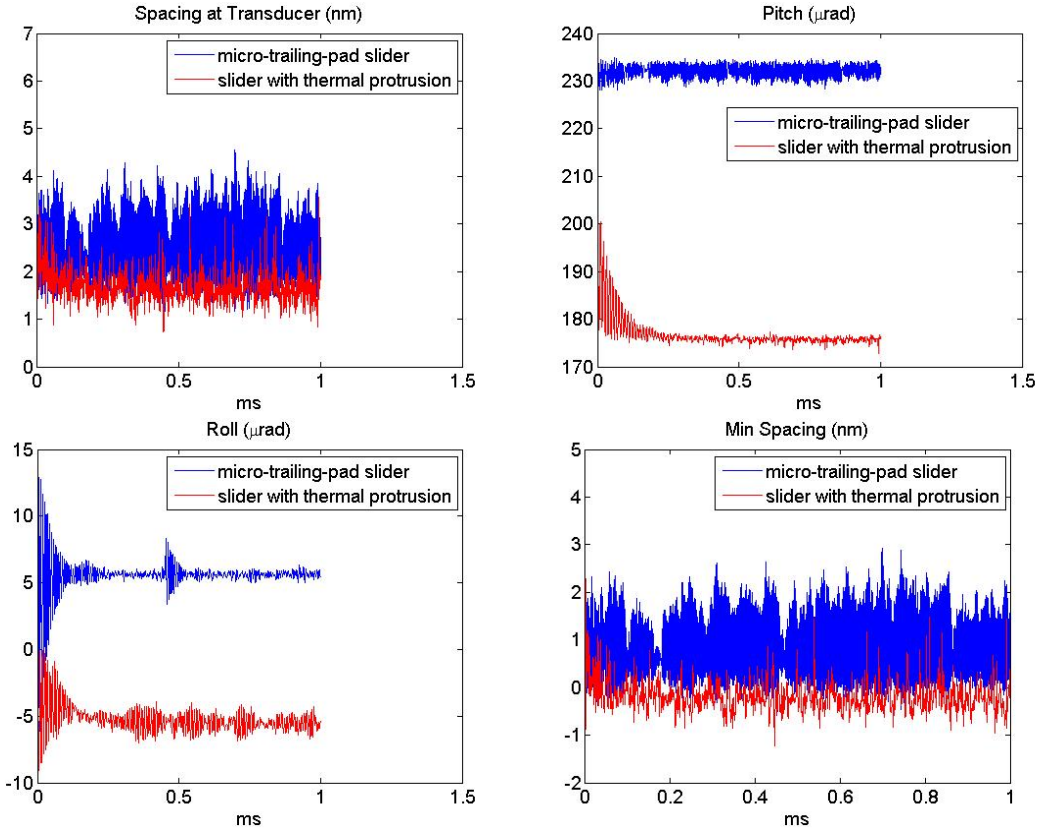

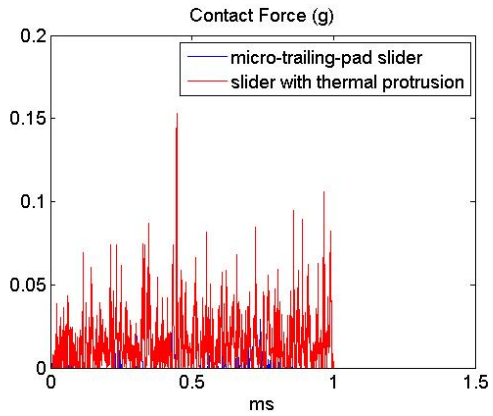

Fig.4. Time histories of a partial contact slider with thermal protrusion and a partial contact micro-trailing-pad slider on the smooth track.

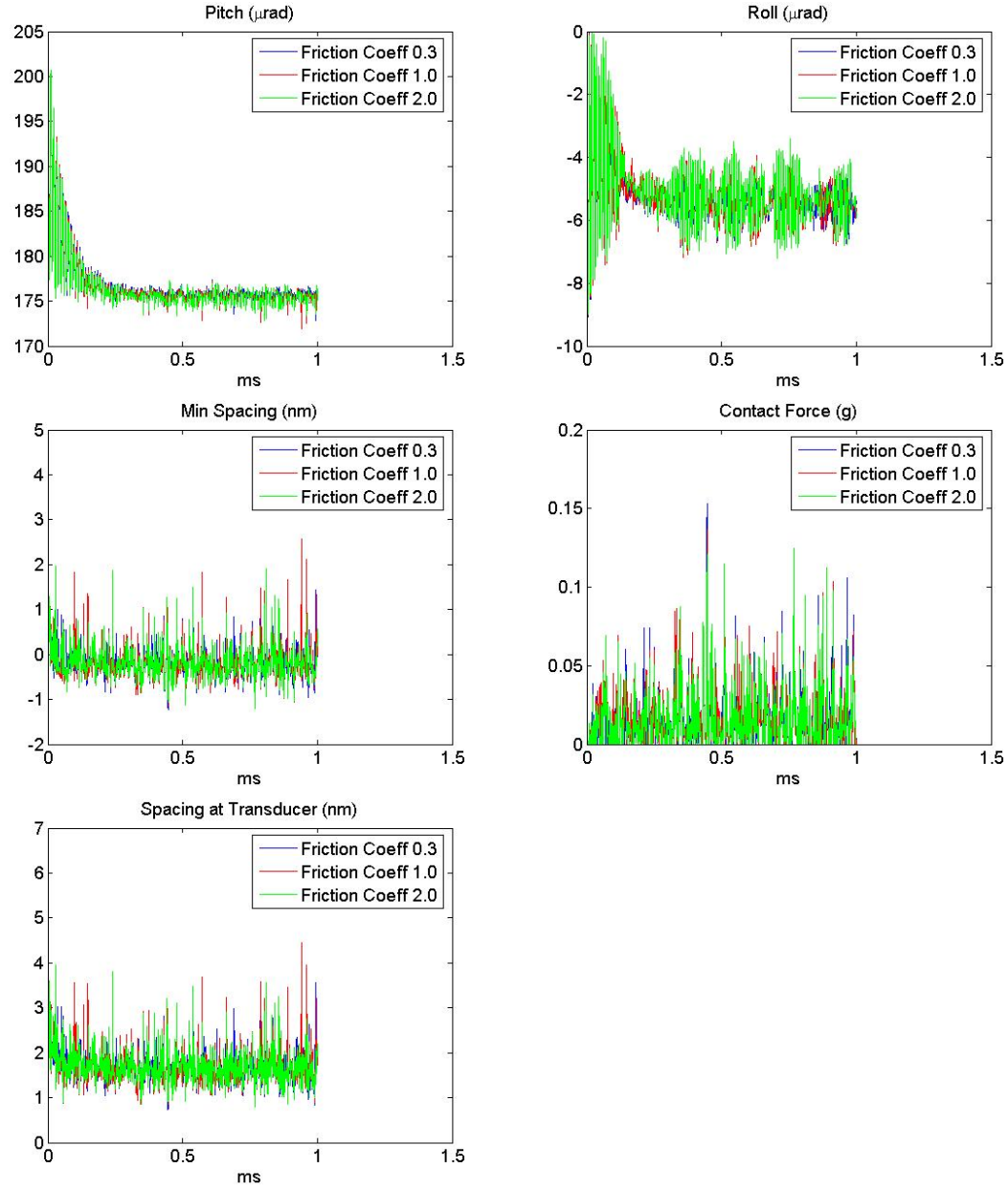

Fig.5. Time histories of Slider 1 with 25 mW heating power on the smooth disk track with the friction coefficient values of 0.3, 1.0 and 2.0.

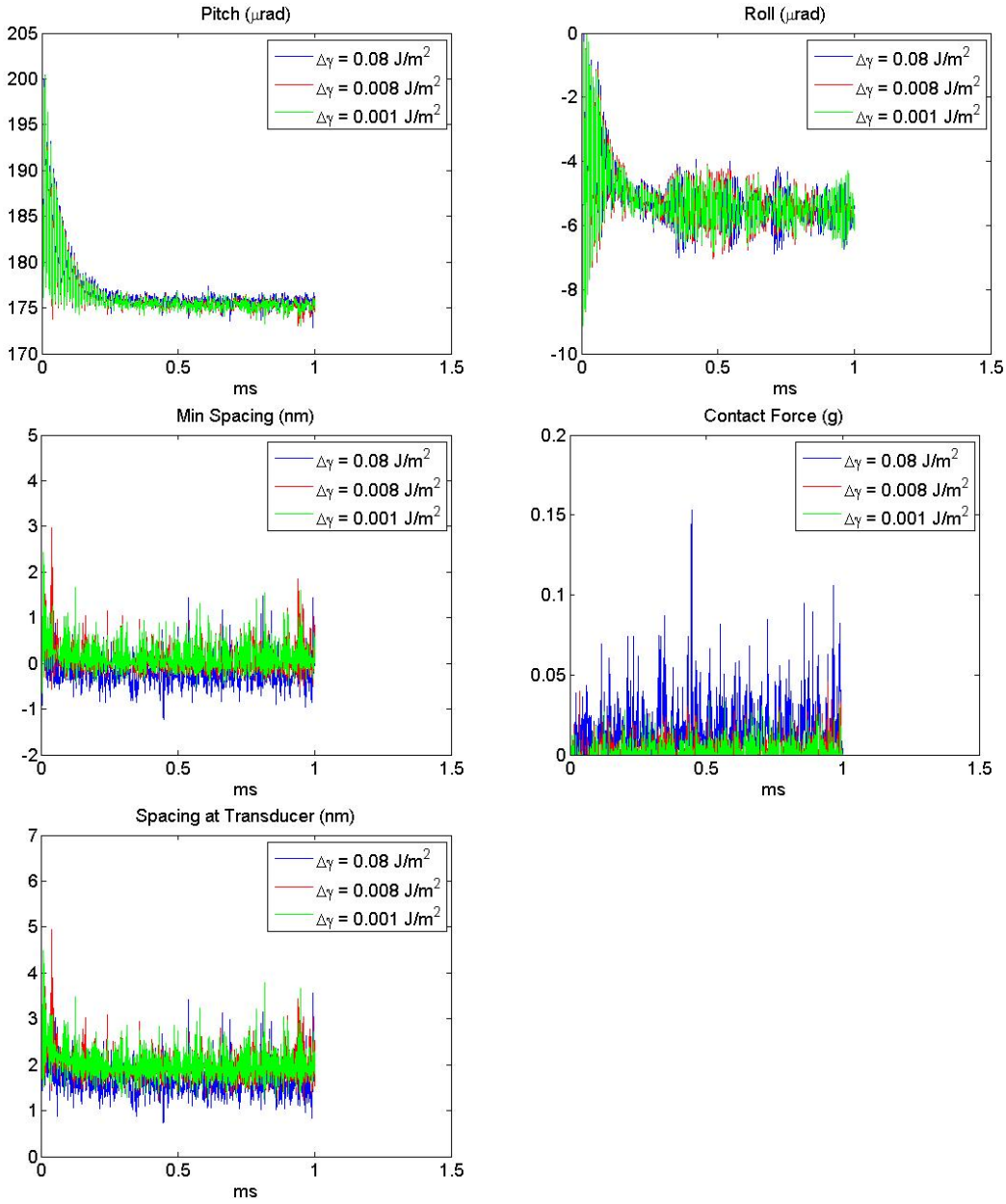

Fig.6. Time histories of Slider 1 on the smooth track with the change of surface energy before and after slider-disk contact ($\Delta\gamma$) for values of 0.08 J/m^2, 0.008 J/m^2 and 0.001 J/m^2.

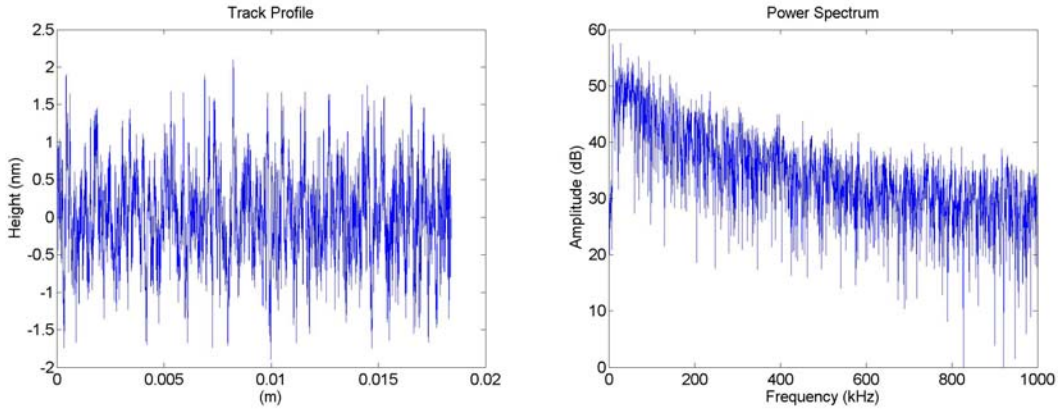

Fig.7. A rough disk track profile and its power spectrum corresponding to a disk linear velocity of 17.34 m/s.

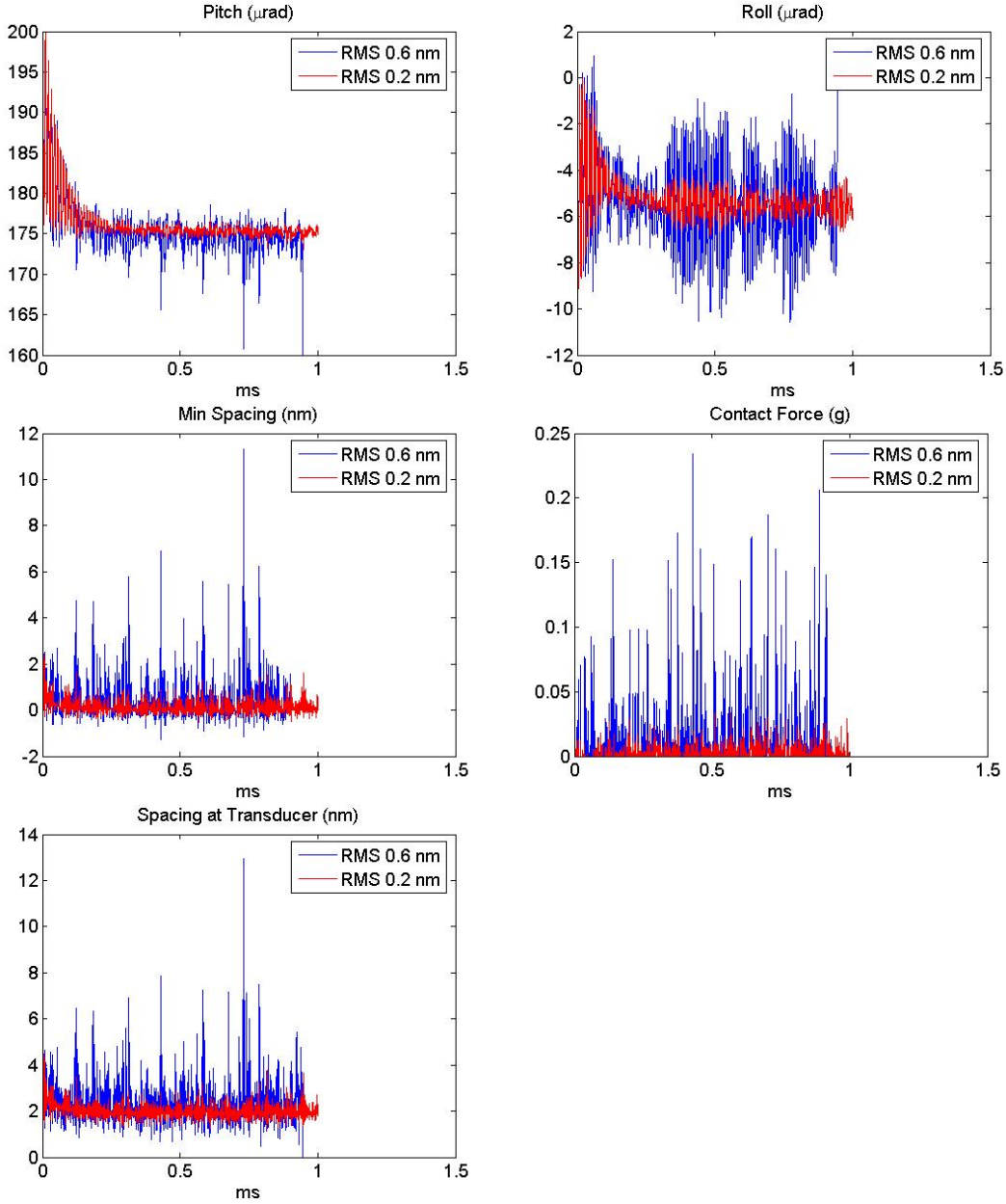

Fig.8. Time histories of Slider 1 with 25 mW heating power on the smooth track and

the rough track.

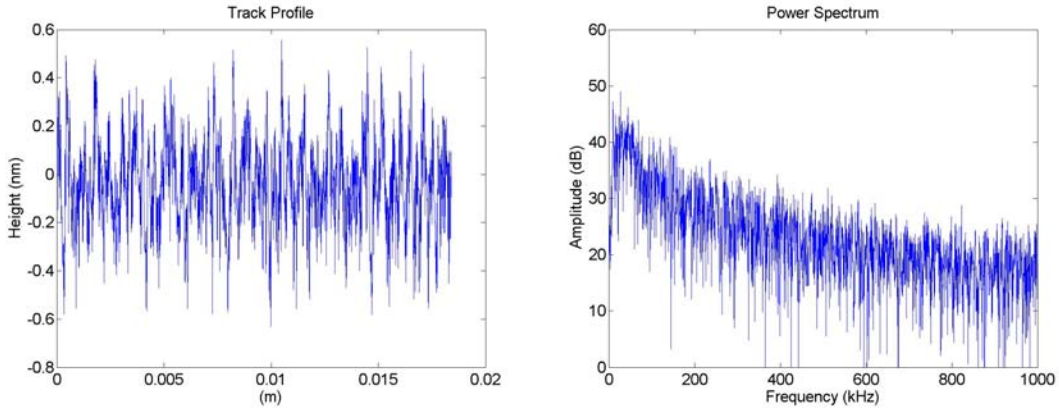

(a) Time-domain burnished track profile and its power spectrum corresponding to a linear velocity of 17.34 m/s.

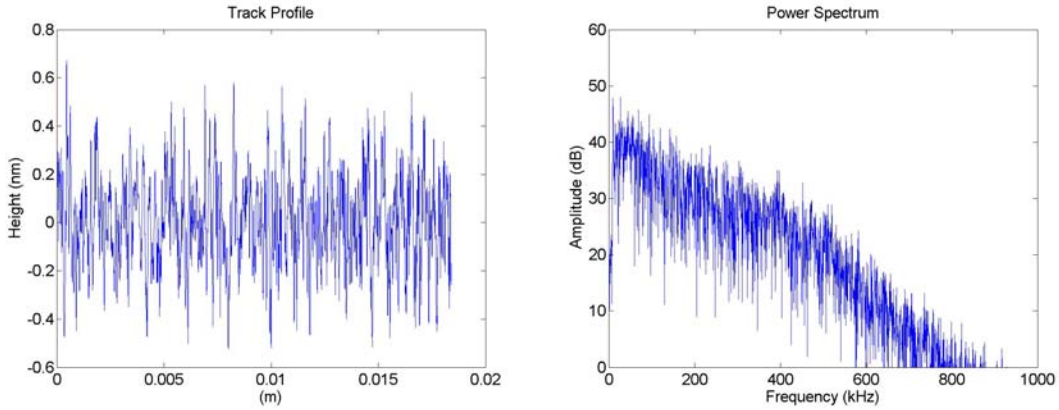

(b) Frequency-domain burnished track profile and its power spectrum corresponding to a linear velocity of 17.34 m/s.

Fig.9. Burnished track profiles and their power spectra corresponding to a disk linear velocity of 17.34 m/s

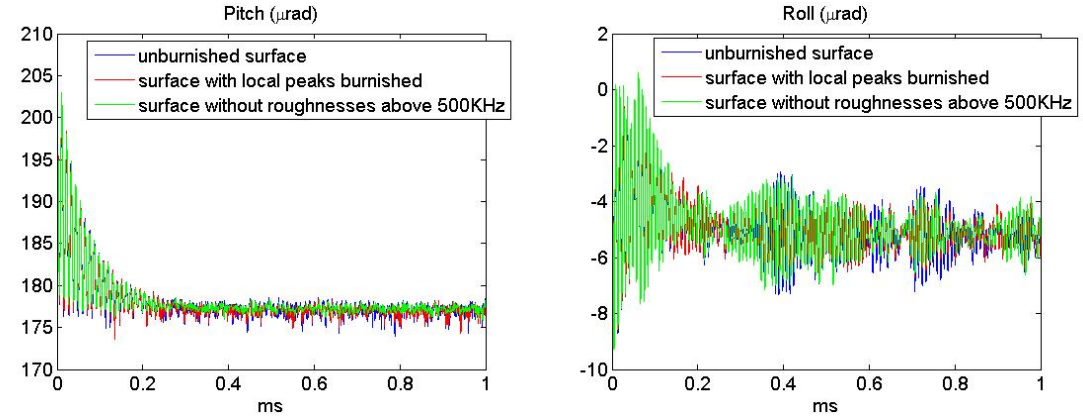

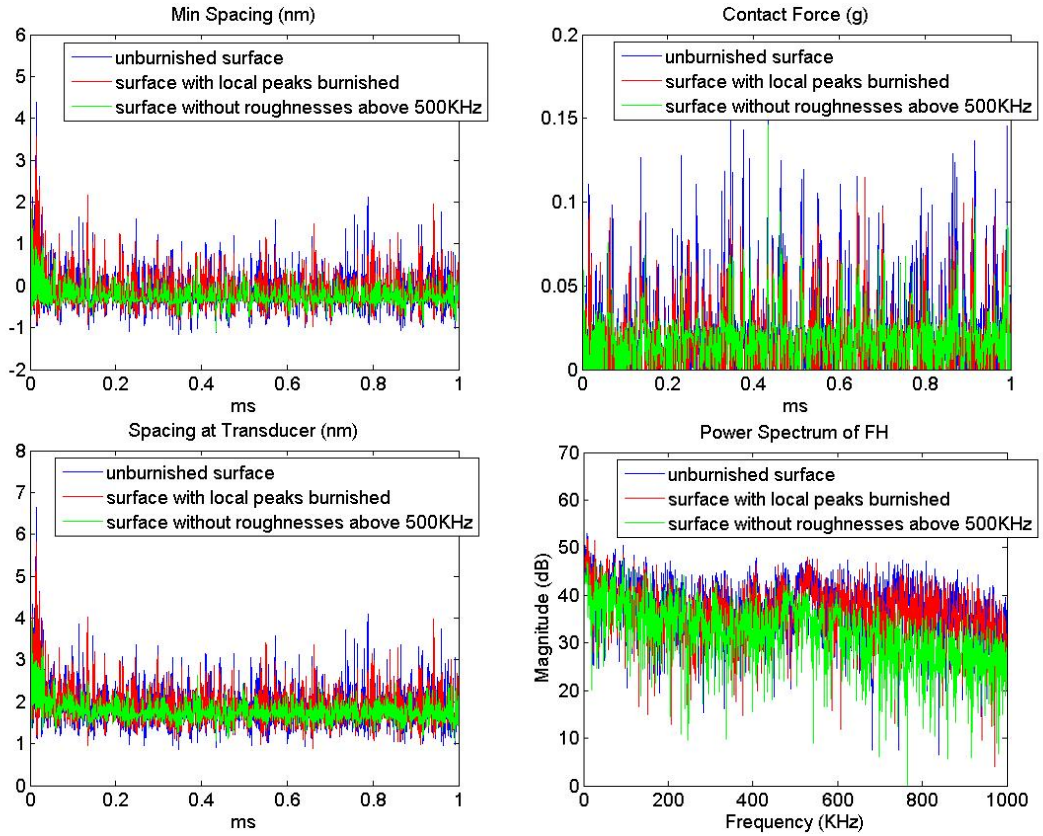

Fig.10. Time histories of Slider 1 on the smooth track (shown in Fig.2.) and burnished tracks (shown in Fig.9.) and the corresponding power spectra of FH.

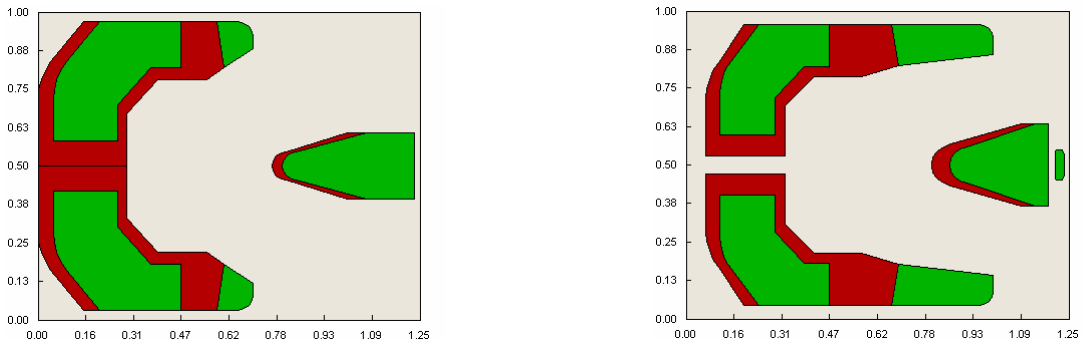

(a) Slider 2 (b) Slider 3

Fig.11. Air bearing surfaces of Slider 2 and Slider 3 (unit: mm).

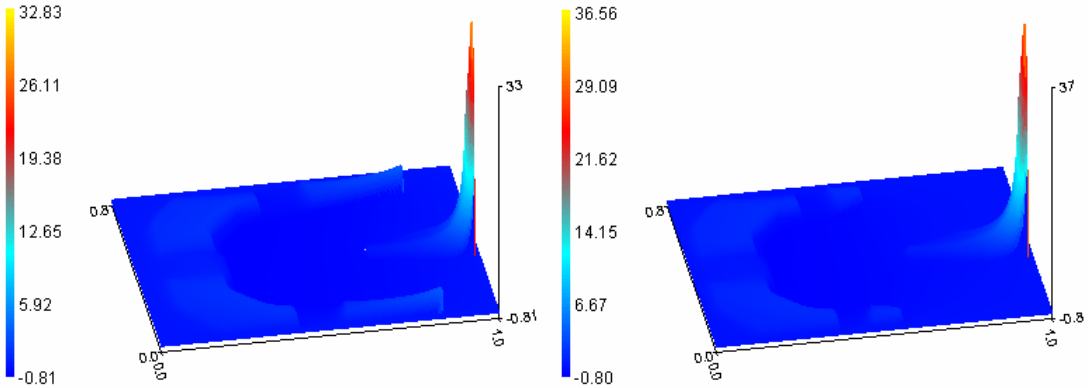

(a) Slider 1 (b) Slider2

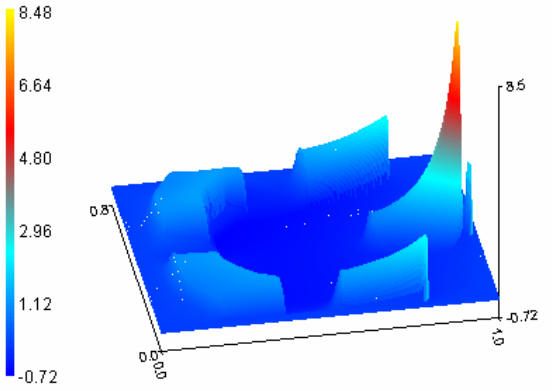

(c) Slider 3

Fig.12. Air bearing pressure profiles of Slider 1, 2 and 3, respectively, at the static state with heating power off (unit: atm).

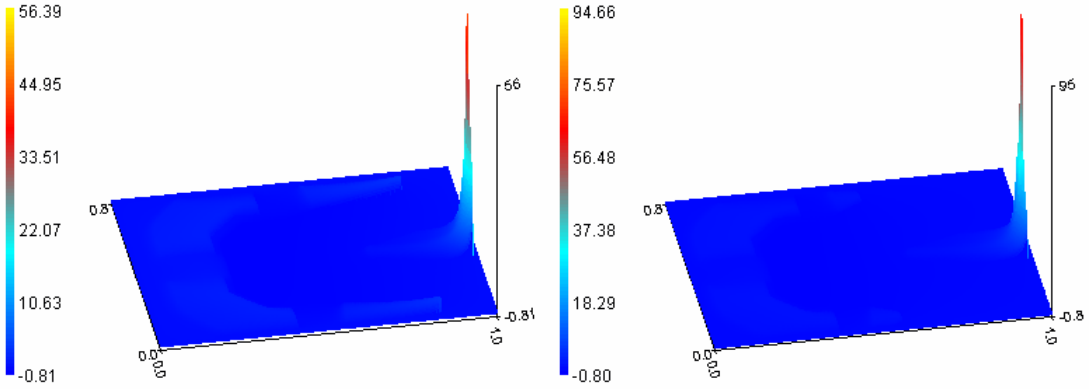

(a) Slider 1 (b) Slider 2

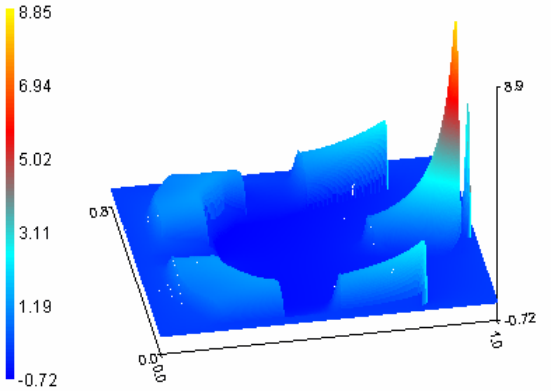

(c) Slider 3

Fig.13. Air bearing pressure profiles of Slider 1, 2 and 3, respectively, at the static state with the touch-down heating power (unit: atm).

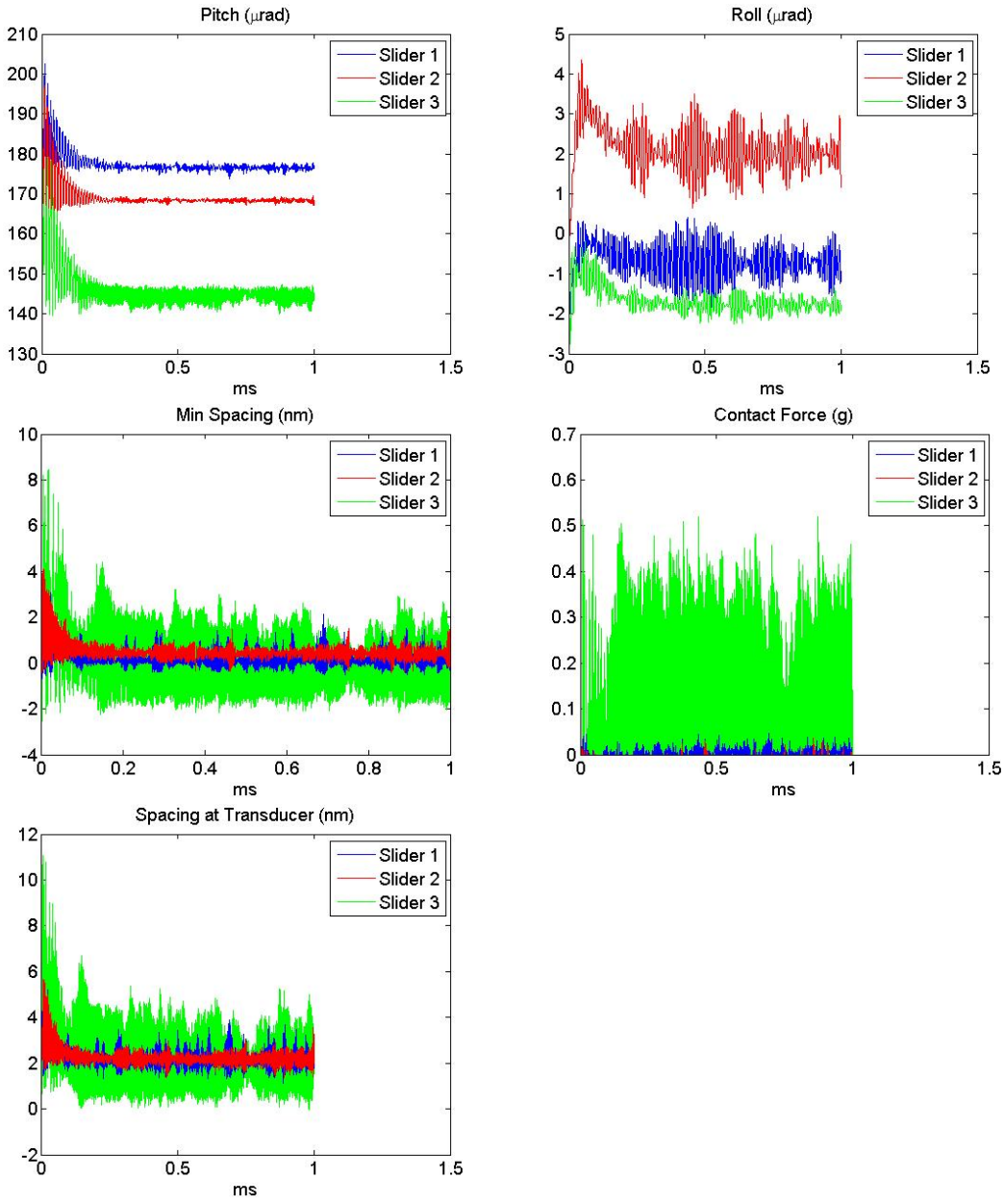

Fig.14. Time histories of the slider dynamics on the smooth track for Slider 1, 2 and 3.